Raman spectrum of gadolinium molybdate at 80°K†

B. N. Ganguly,*‡ Frank G. Ullman, R. D. Kirby, and J. R. Hardy
Behlen Laboratory of Physics, University of Nebraska, Lincoln, Nebraska 68508
(Received 9 June 1975)

Lines that overlap from thermal broadening in the room-temperature Raman spectrum of gadolinium molybdate are resolved in the 80°K spectrum. A total of 126 of the possible 201 lines have been resolved. Symmetry assignments are derived from considerations of both point symmetry and polariton dispersion, supported by separate measurements of A_1(TO) and A_1(LO) spectra. The splitting of the unstable 47 cm^{-1} room-temperature A_1(TO) line into a doublet at 44.5 and 51.5 cm^{-1}, observed previously only in ir absorption, is also observed in these spectra. On heating, the 44.5-cm^{-1} line remains fixed in frequency whereas the 51.5-cm^{-1} line broadens and shifts toward lower frequency until, above 210°K, the 44.5-cm^{-1} line is obscured. Another A_1(TO) line, peaking at 83 cm^{-1} at 80°K, shifts toward lower frequency on heating, reaching 75 cm^{-1} at room temperature and remaining at that value on further heating up to the transition at 159°C where it becomes Raman inactive. The broadening of the 51.5-cm^{-1} line in the A_1(LO) spectrum is less pronounced so its correlation with the modes of the high-temperature phase can be determined unambiguously. These three lines are suggested to be associated with a system of three coupled modes, whose behavior is discussed, qualitatively, in terms of energy transfer between modes and damping via a two-phonon decay involving an optic phonon of about 44.5 cm^{-1} and a long-wave acoustic phonon.

I. INTRODUCTION

The Raman spectrum of gadolinium molybdate, $Gd_2(MoO_4)_3$, has been studied previously at room temperature and above its 159 °C ferroelectric transition.[1] Of a possible 201 Raman-active modes in the ferroelectric phase, only 68 could be identified. Since many of the calculated phonon energies were found to be closely spaced[2] and the anomalous, room-temperature 47-cm^{-1} A_1 mode[3,4] had been reported to split into a doublet at low temperature,[5] it was clear that further resolution and identification would be forthcoming from measurements of the Raman spectrum at lower temperature. In this paper, the spectrum measured at 80 °K is described and classified. In addition, the effect of heating from 80 °K on the three lowest-frequency A_1 lines, that appear to be associated with the ferroelectric transition, is described and interpreted.

In the room-temperature spectrum, described previously,[1] some lines appeared in more than one symmetry. The symmetry assignment for a given line was taken to be the one in which the line appeared with the highest intensity. The appearance of lines of the same frequency in other symmetries was thought to result from "leakage" (from misalignment and the effect of the collecting angle of the focusing lens) from the orientation in which it appeared with highest intensity. In the work described here, examination of the changes in the spectrum with small changes in crystal alignment showed clearly which lines could be attributed to leakage; in practically all cases, leakage could be ruled out as a source of the observed degeneracies. That such degeneracies exist is not surprising: not only in view of the close spacing of the calculated phonon frequencies[2] but also because of the nearly horizontal slope of many of the dispersion curves.[2] Because of the latter, the zone-boundary phonons of the high-temperature phase that become zone-center phonons in the low-temperature phase because of the cell doubling, may be degenerate with the zone-center phonons that are common to both phases. Consequently, in this work all observed lines other than the few leakage lines are assumed to be genuine and are classified accordingly.

In the ferroelectric phase, $Gd_2(MoO_4)_3$ is orthorhombic (C_{2v}) with 68 atoms/cell. All of the 201 optic phonons are Raman active. The Raman tensors and mode classifications for both phases of $Gd_2(MoO_4)_3$ are shown in Table I. It can be seen that there are 50 A_1, 51 A_2, 50 B_1, and 50 B_2 optic modes. Of these, 108 are internal modes, i.e., they are associated with coupled, internal vibrations of the MoO_4^{--} ions. The remaining 93 external modes are subdivided into 23 A_1, 24 A_2, 23 B_1, and 23 B_2.[6] Since the A_1, B_1, and B_2 symmetries are also ir active and $Gd_2(MoO_4)_3$ is noncentrosymmetric, special care must be taken in the selection of the Raman-scattering geometry to ensure that the phonon propagation is along a symmetry axis. If it is not, mode mixing due to polariton angular dispersion[7] can occur and complicate the process of identification of the Raman-line symmetries.

II. EXPERIMENTAL DETAILS

Raman spectra were measured with a Spex model 1401 double monochromator, with about 1.0 – cm^{-1}

spectral resolution. The excitation source was a Coherent Radiation Laboratory Model 52 argon-ion laser. Both the 4880- and 5145-Å lines were used with input powers of 500 mW. The signal was detected with a thermoelectrically-cooled EMI 9502 BA photomultiplier tube along with standard photon-counting electronics.

The samples were cut from a c-axis boule purchased from the Isomet Corporation. All samples were cut into cubes 6 mm on a side with their faces parallel to the orthorhombic crystallographic axes.

The samples were mounted on a cold finger in a conventional liquid-nitrogen optical Dewar. A nominal 300-Ω heater coil of enamel-coated 40-gauge manganin wire was wrapped around a copper sample holder and thermally anchored with GE 7031 varnish. The temperature was measured with a resistance thermometer consisting of a 0.1-W carbon resistor with a resistance of 4750 Ω at 300 °K connected to a Wheatstone bridge and null detector. Temperature variations of 0.5 °K could be detected over the entire range.

III. EXPERIMENTAL RESULTS

The identifications of the Raman lines according to the point symmetries of the corresponding pho-

TABLE I. (a) Symmetry correlation of the low- and high-temperature phases [J. Petzelt and V. Dvorak, Phys. Status Solidi B 46, 413 (1971)]; (b) Raman tensors for the two phases [R. Loudon, Adv. Phys. 13, 423 (1964)].

(a)

ORTHORHOMBIC PHASE C_{2d}^8			TETRAGONAL PHASE D_{2d}^3		
SYMMETRY TYPE	INFRARED ACTIVITY	RAMAN ACTIVITY	SYMMETRY TYPE	INFRARED ACTIVITY	RAMAN ACTIVITY
		α_{zz}	A_1	---	$\alpha_{zz}, \alpha_{xx}, \alpha_{yy}$
A_1	$\vec{E}\|\|\vec{Z}$	α_{xx}	B_2	$\vec{E}\|\|\vec{Z}$	$\alpha_{xx}-\alpha_{yy}$
		α_{yy}	T_1	---	---
			A_2	---	---
A_2	---	α_{xy}	B_1	---	α_{xy}
			T_2	---	---
B_1	$\vec{E}\|\|X$	α_{xz}	E	$\vec{E}\|\|(x,y)$	$(\alpha_{yz}, \alpha_{xz})$
B_2	$\vec{E}\|\|y$	α_{yz}	τ_5		

(b)

$C_{2v}(nm2)$ $\begin{pmatrix} a & 0 & 0 \\ 0 & b & 0 \\ 0 & 0 & c \end{pmatrix}$ $\begin{pmatrix} 0 & d & 0 \\ d & 0 & 0 \\ 0 & 0 & 0 \end{pmatrix}$ $\begin{pmatrix} 0 & 0 & e \\ 0 & 0 & 0 \\ e & 0 & 0 \end{pmatrix}$ $\begin{pmatrix} 0 & 0 & 0 \\ 0 & 0 & f \\ 0 & f & 0 \end{pmatrix}$

$A_1(z)$ A_2 $B_1(x)$ $B_2(y)$

$D_{2d}(\bar{4}2m)$ $\begin{pmatrix} d & 0 & 0 \\ 0 & a & 0 \\ 0 & 0 & b \end{pmatrix}$ $\begin{pmatrix} c & 0 & 0 \\ 0 & -c & 0 \\ 0 & 0 & 0 \end{pmatrix}$ $\begin{pmatrix} 0 & d & 0 \\ d & 0 & 0 \\ 0 & 0 & 0 \end{pmatrix}$ $\begin{pmatrix} 0 & 0 & e \\ 0 & 0 & 0 \\ e & 0 & 0 \end{pmatrix}$ $\begin{pmatrix} 0 & 0 & 0 \\ 0 & 0 & e \\ 0 & e & 0 \end{pmatrix}$

A_1 B_1 $B_2(z)$ $E(y)$ $E(x)$

non modes can be made from inspection of the equation for the scattering efficiency[8]

$$S = A(\epsilon_\sigma R_{\sigma\rho}\epsilon_\rho)^2, \quad \sigma, \rho = x, y, z, \tag{1}$$

where $R_{\sigma\rho}$ is the appropriate Raman tensor for the crystal class, ϵ_σ and ϵ_ρ are the components of the unit vectors characterizing incident and scattered beam polarizations, respectively, and A is a proportionality constant.

For infrared-active phonons in a biaxial crystal such as $Gd_2(MoO_4)_3$, this identification is not, in general, valid. Since the A_1, B_1, and B_2 modes are infrared active, the Raman spectrum for a given point symmetry will depend on the phonon propagation direction. To analyze such cases properly, the polariton dispersion relation should be used. For large-angle scattering, where the polariton velocity is small compared to the velocity of light in the medium, the polariton dispersion relation reduces to[7]

$$\epsilon_1 q_1^2 + \epsilon_2 q_2^2 + \epsilon_3 q_3^2 = 0, \tag{2}$$

where the q_i are the components of the phonon propagation vector and the ϵ_i are principal-axis dielectric functions, given by

$$\epsilon_i = \epsilon_1^\infty + \sum_{j=1}^{50} \frac{s_j}{\omega_{0j}^2 - \omega^2} \ . \tag{3}$$

Here, s_j is the oscillator strength and ω_{0j} is the TO frequency of the jth mode that contributes to the i-axis dielectric function.

The right-angle scattering geometries used in these measurements were $x(zz)y$, $x(yx)y$, $x(zy)z$, and $y(zx)z$ which from Eqs. (1)–(3) can be shown to correspond, respectively, to $A_1(z)$, A_2, $B_2(y)$, and $B_1(x)$ symmetries. It was important in this work to obtain the A_1(TO) and A_1(LO) spectra separately.

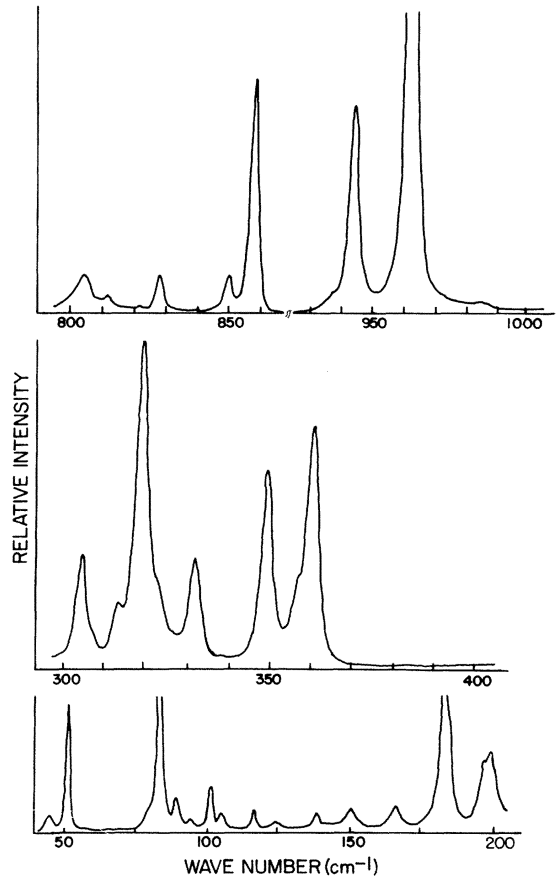

FIG. 1. A_1(TO) spectra, $x(zz)y$, 80 °K (a weak line at 210 cm^{-1} is not shown).

TABLE II. Observed A_1 lines ($T < T_c$) and corresponding lines of the high-temperature (D_{2d}) phase in cm^{-1} (sh, shoulder; bo, barely observable).

A_1		
LO	TO	D_{2d}
44.5	44.5	T_1
52	51.5	50.0 B_2
83	83	T_1
89.5	89.5	90 A_1
94	94	94 A_1
101	101	97 B_2
105	105	T_1
116	116	111 B_2
124	123	T_1
138	138	T_1
150	150	144 B_2
161	161 sh	160 B_2
170	165	T_1
188	183	182 A_1
198	198	194 B_2
230	210	T_1
308	306	298 B_2
315	315 sh	308 B_2
323	320	320 A_1
326	324 sh	320 B_2
332	332	T_1
353	350	350 A_1
364	358	360 A_1
368	362	360 B_2
387	380	380 B_2
808	805	796 B_2
815	812	807 B_2
816	815	818 A_1
820	818 bo	818 B_2
823	822	822 B_2
831	828	830 A_1
852	850	847 B_2
860	858	855 A_1
936	936	T_1
945	944	940 A_1 or 941 B_2
963	962	960 A_1 or 954 B_2
974	972	T_1

From Eq. (2), it can be seen that to obtain only an LO-phonon spectrum the phonon propagation direction must be along a principal axis. Consequently the A_1(LO) spectrum was studied in the backscattering configuration $z(xx)\bar{z}$.

The Raman lines fall into two spectral groupings, 0–400 and 740–1000 cm^{-1}. From an examination of the figures and tables, discussed below, it can be seen that a few lines that can be seen in the figures have not been tabulated. We have included in the tables only those lines that can be identified unequivocally as part of the first order spectrum. (Identification of weak lines always involves some degree of uncertainty since they may be artifacts from electrical or optical noise, leakage from other symmetries, or of higher order.) In the A_1 spectra, we have applied the additional restriction that *pairs* of TO and LO lines had to appear reproducibly. The lines that can be seen at 119, 181, 298, and 312 cm^{-1} and between 230 and 280 cm^{-1} did not satisfy this last criterion.

The A_1(TO) and A_1(LO) spectra (all at 80 °K) are

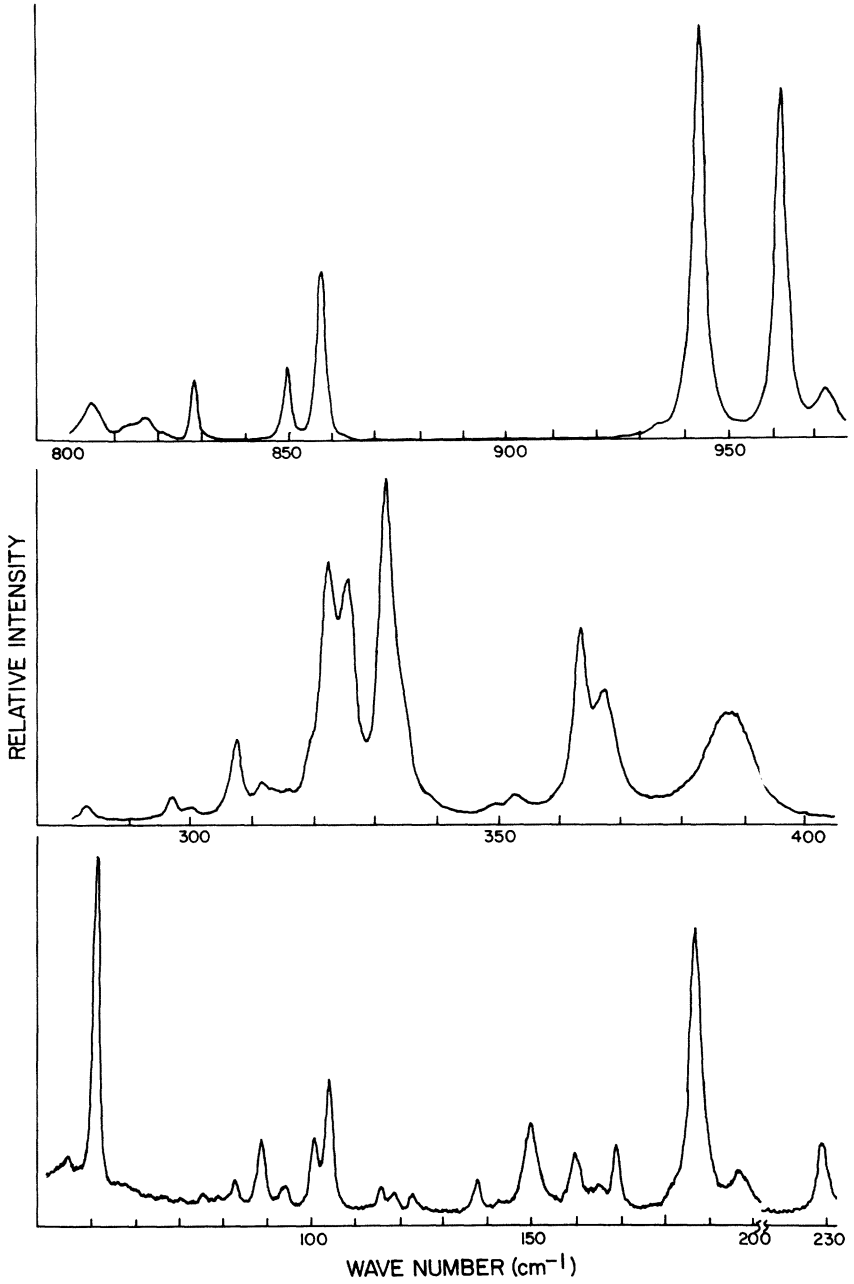

FIG. 2. A_1(LO) spectra, $z(xx)\bar{z}$, 80 °K.

shown in Figs. 1 and 2, respectively, B_1 spectra in Fig. 3, B_2 spectra in Fig. 4, and A_2 spectra in Fig. 5.

In Tables II–V, the frequencies of all the first-order lines are listed along with their correlation with corresponding lines[1] from the high-temperature phase. (Some of these high-temperature lines were excluded in our earlier work.[1]) Identification of the D_{2d} phonons that correlate with C_{2v} phonons of A_2 symmetry poses a special problem because A_2 modes are not Raman observable in the D_{2d} phase and, thus, whether or not the correlation is with an A_2 or a zone-boundary phonon is not apparent. The polarizability changes associated with the zone-boundary, T_2 modes are likely to be small compared to those associated with the Raman-inactive A_2 modes. Therefore, strong A_2 lines are identified here as A_2 in the D_{2d} phase; otherwise, they are listed as either "A_2 or T_2."

An A_1 (TO) line, 47 cm^{-1} at room temperature,

TABLE III. Observed B_1 lines ($T < T_c$) and corresponding lines of the high-temperature (D_{2d}) phase in cm^{-1}.

B_1	D_{2d}	B_1	D_{2d}
43.0	τ_5	328.0	τ_5
50.5	50.0 E	335.0	τ_5
64.0	τ_5	341.0	341.0 E
91.0	90.0 E	382.0	380.0 E
98.0	τ_5	404.0	404.0 E
112.0	τ_5	740.0	742.0 E
136.0	130.0 E	745.0	τ_5
141.5	E	822.0	817.0 E
169.5	160.0 E	838.0	τ_5
187.0	E	844.0	835.0 E
200.0	190.0 E	848	844.0 E
285.0	279.0 E	857.0	τ_5
292.0	τ_5	911.0	915.0 E
300.0	τ_5	939.0	930.0 E
309.0	306.0 E	957.0	965.0 E
320.0	325.0 E		

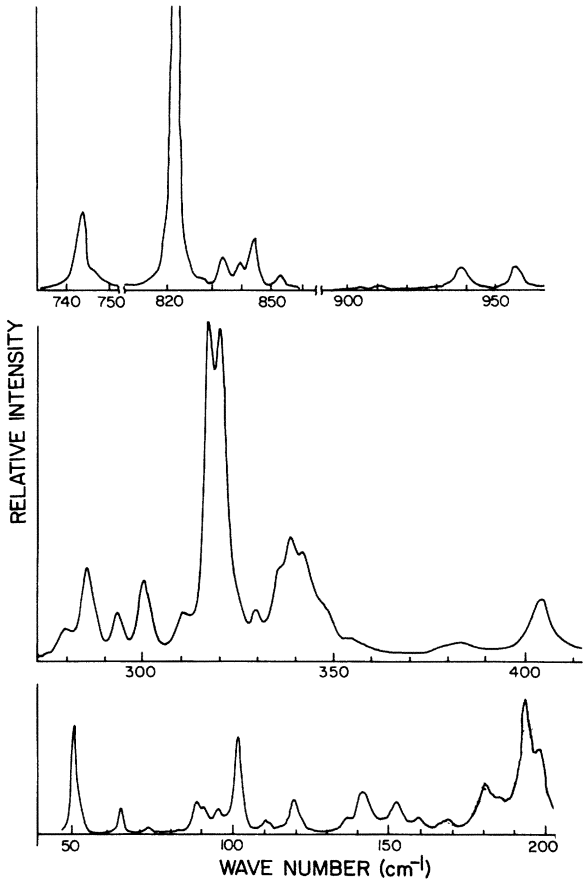

FIG. 3. B_1 spectra, $x(zy)z$, 80 °K.

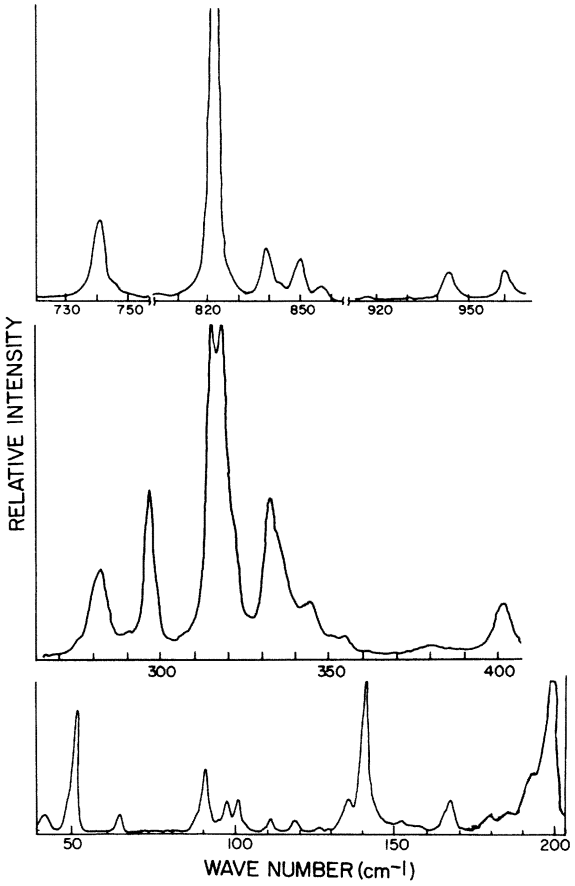

FIG. 4. B_2 spectra, $y(zx)z$, 80 °K.

whose peak frequency decreases on heating has been observed previously in $Gd_2(MoO_4)_3$.[3] Also, two overlapping A_1(TO) modes have been observed in infrared absorption[5] at low temperatures which coalesce into one broad line at room temperature, peaking at about 47 cm^{-1}. Both the temperature[3] and stress[4] dependence above room temperature of this anomalous line are not exactly reproduced by a simple Lorentzian line.

We have reported briefly on the A_1 spectrum below 100 cm^{-1} previously.[9] A_1(TO) spectra up to 100 cm^{-1} for four different temperatures between 80 and 300 °K are shown in Fig. 6. It can be seen that the 51.5-cm^{-1} peak frequency decreases with increasing temperatures while its linewidth increases. This line has coalesced with the 44.5-cm^{-1} line at room temperature, just as observed in infrared absorption.[7] The peak frequency of the 44.5-cm^{-1} line did not shift up to the highest temperature at which this line could still be resolved.

The peak frequency of the 83-cm^{-1} line also decreased with increasing temperature to a value of 75 cm^{-1} at room temperature and remains at this value on heating up to the transition where it becomes Raman inactive (zone boundary mode), as shown in Fig. 7 (taken from Ref. 10).

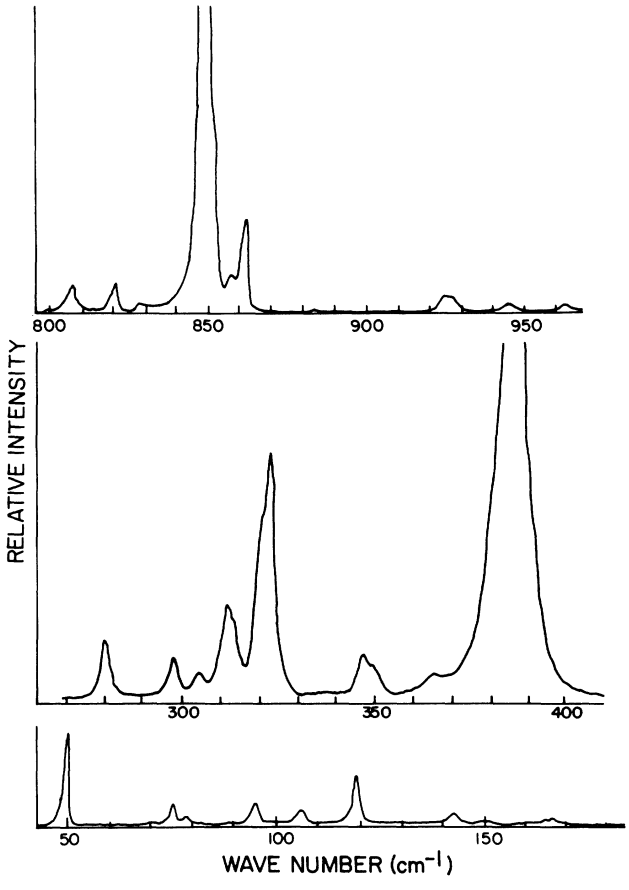

FIG. 5. A_2 spectra, $x(yx)y$, 80 °K.

TABLE IV. Observed B_2 lines ($T < T_c$) and corresponding lines of the high-temperature (D_{2d}) phase in cm^{-1}.

B_2	D_{2d}	B_2	D_{2d}
49.0	50.0 E	332.0	341.0 E
64.0	τ_5	334.0	τ_5
95.0	τ_5	354.0	τ_5
101.0	90.0 E	379.0	380.0 E
110.0	τ_5	402.0	404.0 E
120.0	130.0 E	740.0	742.0 E
152.0	E	745.0	τ_5
159.0	160.0 E	820.0	817.0 E
180.0	E	840.0	835.0 E
194.0	190.0 E	844.0	τ_5
272.0	279.0 E	851.0	844.0 E
290.0	τ_5	857.0	τ_5
296.0	306.0 E	916.0	915.0 E
315.0	325.0 E	944.0	930.0 E
320.0	τ_5	962.0	965.0 E

A_1(LO) spectra up to 100 cm^{-1}, taken in the $z(xx)\bar{z}$ configuration, are shown in Fig. 8 for several temperatures from 80 up to 425 °K. [Spectra for above room temperature were measured by one of us (BNG) in the UCLA Chemistry laboratories.] As in the TO spectra, the 44.5-cm^{-1} line is obscured above room temperature by the broadening of the 51.5-cm^{-1} line. However, the damping is much weaker in LO than in TO; the 51.5-cm^{-1} line does not damp into the background below T_c as in the TO spectrum. In fact, the intensity of the 51.5-cm^{-1} line increases with temperature whereas the

TABLE V. Observed A_2 lines ($T < T_c$), and corresponding lines of the high-temperature (D_{2d}) phase in cm^{-1}.

A_2	D_{2d}	A_2	D_{2d}
51	50 B_1	314.0	T_2
76	A_2 or T_2	322	T_2
79.0	A_2 or T_2	323	326.0 B_1
95.0	94.0 B_1	348	A_2
106.0	A_2 or T_2	350	T_2
119.0	114.0 B_1	366	T_2
142.5	144.0 B_1	387	385.0 B_1
70.5		809	A_2
150.0	A_2 or T_2	822	A_2
166.0	162.0 B_1	830	T_2
281	286.0 B_1	850	851.0 B_1
299	A_2	858	T_2
305	T_2	926	921.0 B_1
312.0	318.0 B_1	929	T_2

intensities of others such as the 83-cm^{-1} line (75 cm^{-1} above 300 °K) decrease as the transition is approached. There is another important difference between these A_1(TO) and A_1(LO) spectra; the former remain A_1 above T_c since the "zz" polarizations are retained whereas the latter go from "xx" to "xy, xy," which corresponds to $A_1+B_1+B_2$ symmetry. From Table I, it can be seen that A_1 phonons of the low-temperature phase transform to A_1, B_2, or T_1 phonons in the high-temperature phase. There are no lines near 50 cm^{-1} in the A_1 spectrum above T_c. There is[1] a strong B_2 line at 50 cm^{-1}, and since according to Table I, B_2 modes above T_c must have corresponding A_1 modes but no corresponding modes of other symmetries below T_c, the 51.5-cm^{-1} line must be a zone-center mode in both phases, going from A_1 to B_2 on heating through T_c. The 44.5- and 83-cm^{-1} lines do not appear in either A_1 or B_2 spectra above T_c and, therefore, must become T_1 zone-boundary modes.

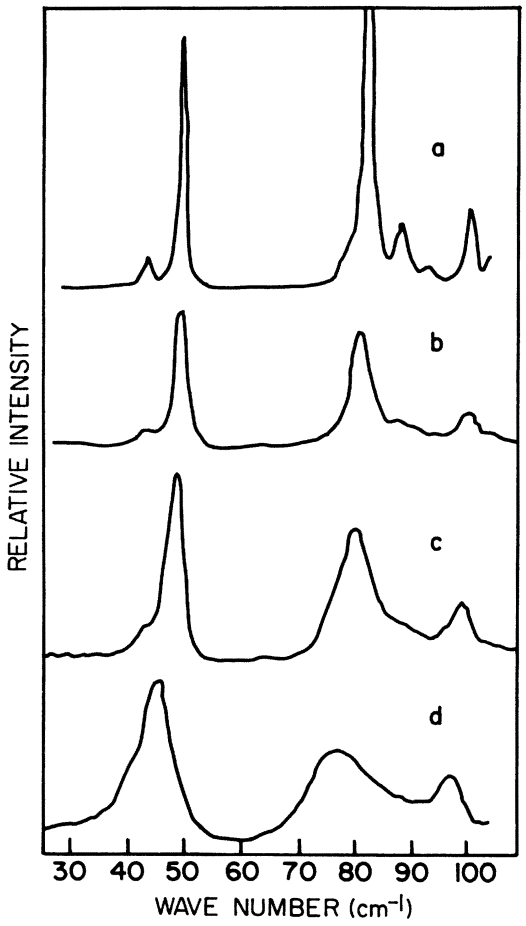

FIG. 6. A_1(TO) spectra, 0–100 cm^{-1}, for four temperatures: (a) 80 °K, (b) 160 °K, (c) 210 °K, and (d) 300 °K.

These, then, are the likely candidates for the two A_1 lines below T_c that correspond to the two soft degenerate zone-boundary modes above T_c, as we have suggested previously.[9]

IV. DISCUSSION OF RESULTS

By cooling to 80 °K, it has been possible to resolve 126 of the possible 201 Raman-active modes. Among these, the behavior of the A_1 spectrum below 200 cm^{-1} is of most interest since it contains the only spectral features exhibiting abnormal temperature dependence. The ferroelectric phase transition has been shown[11] to originate from the softening of two degenerate zone-boundary phonons on cooling to T_c. Below T_c, this degeneracy is removed and the two soft phonons become Raman-active A_1 modes. These have not been identified unequivocally; in fact, the behavior below T_c has not yet been elucidated. The explanation of the lattice dynamics of the ferroelectric phase will have to account for the anomalous damping of certain modes,[3,4,9] the absence of a dielectric anomaly,[12] the existence of anomalies in some of the elastic constants,[13] and the ferroelasticity.[14]

If the Lyddane-Sachs-Teller relation is valid for this system, the observed absence of any dielectric anomaly for the clamped crystal must mean that the ratio of the LO to TO frequencies remains fixed, and if there is any softening, the two soften

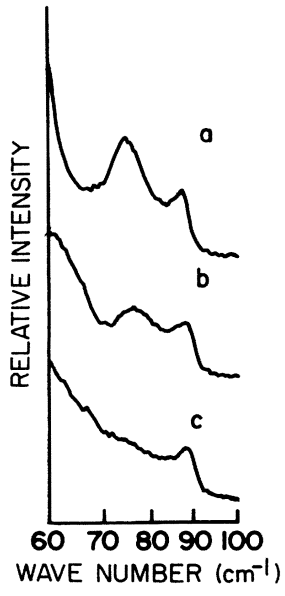

FIG. 7. Behavior of 83-cm^{-1} line (75 cm^{-1} at 300 °K) on heating through T_c: (a) 300 °K, (b) 373 °K< T < 432 °K = T_c, (c) T > 432 °K.

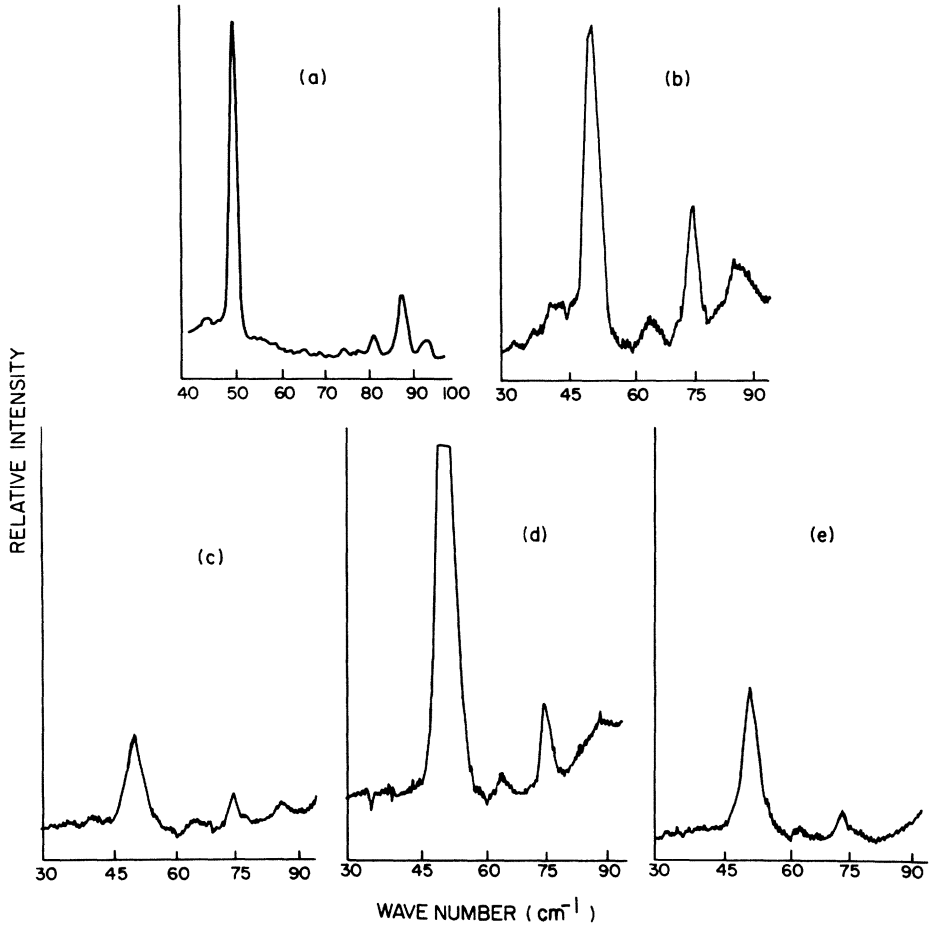

FIG. 8. A_1(LO) spectra at various temperatures. (a) 80 °K, (b) 300 °K, (c) 363 °K, (d) 403 °K, and (e) 425 °K.

together but the TO branch never reaches zero in the temperature range $T \leq T_c$. Dorner *et al.*[11] have suggested this type of behavior among several possible types for the two A_1 modes involved in the ferroelectric transition. This assumption of little or no softening, as observed,[3,4,9] is consistent with the absence of the dielectric anomaly but offers no clue to the observed anomalies in the elastic constants. There is a clue, however, in the anomalous damping of the three coupled modes at 44.5, 51.5, and 83 cm^{-1} (at 80 °K). We have offered a brief explanation of this damping previously[9]; it goes as follows. The 51.5-cm^{-1} A_1(TO) mode that exhibits anomalous damping has been shown from measurements of the LO-phonon scattering to become a B_2 mode above T_c and not a zone-boundary mode; therefore it cannot be one of the modes involved in the transition. From comparisons of the 80 °K spectra with higher-temperature spectra, the 83-cm^{-1} peak can clearly be seen to begin to soften on heating with a large amount of intensity transfer, presumably into the 51.5-cm^{-1} peak, as evidenced by the much more rapid decrease in peak height of the 83-cm^{-1} peak relative to the 51.5-cm^{-1} peak. Since the 51.5-cm^{-1} mode is not softening, it "pins" the upper peak at 75 cm^{-1} above room temperature. The behavior of the 44.5-cm^{-1} mode is not apparent above room temperature since it is obscured by the 51.5-cm^{-1} mode. However, there is no indication that it softens. Since the damping of the 51.5-cm^{-1} mode disappears above T_c, the damping mechanism may be associated with a nest of modes of small wave vector in the vicinity of 44 cm^{-1}, of which the 44.5-cm^{-1} mode is the zero wave-vector limit. We suggest that the damping is due to a two-phonon decay process involving one of these 44-cm^{-1} modes and a long-wave acoustic phonon (~ 5–7 cm^{-1}). This implies a strong peak in the imaginary part of the self-energies of both the 50-cm^{-1} phonon and the acoustic phonon. This, in turn, implies a marked negative shift in the real part of the self-energy for acoustic phonons of lower frequency (< 5–7 cm^{-1}). Thus there will be an anomalous decrease in the associated elastic constant. If no phase transition took place at T_c, the damping and de-

crease in the elastic constant would continue to change with heating. However, the first-order change at T_c in which the 44-cm^{-1} modes move to the zone boundary causes the damping to disappear, and hence an apparent anomaly in the elastic constant. The elastic behavior is thus a consequence of the phase transition rather than one of its causes. There will also be an associated effect on the real part of the self-energy of the 50-cm^{-1} phonon which could explain the failure of the simple Lorentzian fit.[3,4] Specifically, the deviation between the measured and calculated spectra is such that the former is always higher than the latter below the peak and lower above. This is what is expected when the imaginary part of the self-energy shows a strong peak.[15] In these circumstances, the real part will tend to decrease the effective frequency of the Lorentzian below the peak and increase it above. Such an effect would be in qualitative agreement with the observed behavior.

As mentioned above, the absence of any mode softening in the ferroelectric phase is consistent with some of the qualitative temperature dependences of the "soft modes" below T_c suggested by Dorner, Axe, and Shirane[11] and, therefore, should not be regarded as anomalous.

---

†Research sponsored by the Air Force Office of Scientific Research, Office of Aerospace Research, USAF under Grant No. AFOSR 70-1926.

*This work is part of a dissertation submitted by B. N. Ganguly in partial fulfillment of the requirements for the Ph.D. degree.

‡Present address: Dept. of Chemistry, University of California, Los Angeles, Calif. 90024.

[1]F. G. Ullman, B. J. Holden, B. N. Ganguly, and J. R. Hardy, Phys. Rev. B 8, 2991 (1973).

[2]L. L. Boyer and J. R. Hardy, Phys. Rev. B 8, 2205 (1973).

[3]P. A. Fleury, Solid State Commun. 8, 601 (1970).

[4]B. N. Ganguly, F. G. Ullman, J. R. Hardy, and R. D. Kirby, Phys. Rev. B 12, 3783 (1975).

[5]J. Petzelt, Solid State Commun. 9, 1485 (1971).

[6]J. Petzelt and V. Dvorak, Phys. Status Solidi B 46, 413 (1971).

[7]A. S. Barker and R. Loudon, Rev. Mod. Phys. 44, 18 (1972); E. Anda, Solid State Commun. 9, 1545 (1971).

[8]R. Loudon, Adv. Phys. 13, 423 (1964).

[9]B. N. Ganguly, F. G. Ullman, R. D. Kirby, and J. R. Hardy, Solid State Commun. 17, 533 (1975).

[10]B. J. Holden, Ph.D. dissertation (University of Nebraska, 1971) (unpublished).

[11]B. Dorner, J. D. Axe, and G. Shirane, Phys. Rev. B 6, 1950 (1972).

[12]L. E. Cross, A. Fouskova, and S. E. Cummins, Phys. Rev. Lett. 21, 812 (1968).

[13]U. T. Hochli, Phys. Rev. B 6, 1816 (1972).

[14]K. Aizu, J. Phys. Soc. Jpn. 27, 387 (1969).

[15]R. A. Cowley, *Phonons* (Oliver and Boyd, London, 1966), p. 170.